ANALYSIS OF FLOW AND HEAT TRANSFER PERFORMANCE OF DIFFERENT TYPES OF FLOW CHANNELS IN PRINTED CIRCUIT HEAT EXCHANGERS FOR PRE-COOLERS

by

Xin GU, Xin LIU, Hao SUN, Yiwen ZHU, and Yongqing WANG*

School of Mechanical and Power Engineering, Zhengzhou University, Zhengzhou, China

Original scientific paper
https://doi.org/10.2298/TSCI230902072G

The shape of fins in flow channels of printed circuit heat exchangers (PCHE) significantly affects the heat exchanger performance. In the pre-cooler condition of the marine supercritical CO_2 Brayton cycle power generation system, this study focuses on three typical discontinuous flow channel printed circuit heat exchangers. The investigation involves a numerical analysis of flow and heat transfer performance using CFD method. The comparative consequences illuminate that the rectangular fin channel exhibits the optimal heat transfer performance, and temperature drops are 1.18 times and 1.23 times, exceeding those of airfoil and rhombic fin channels, respectively. All three flow channels show different degrees of temperature drop reduction along the direction of fluid-flow. However, the rectangular fin channel demonstrates the worst flow performance, as pressure drops are 16.6 times and 17.8 times, higher than those of airfoil and rhombic fin channels, respectively. By calculating the values of Nu/f and Q/Δp, the comprehensive performance of each flow channel is ranked from high to low airfoil fin channel, rhombic fin channel, and rectangular fin channel. This research provides guidance for optimizing the design and applying PCHE in engineering for marine supercritical CO_2 Brayton cycle pre-coolers.

Key words: *printed circuit heat exchanger, comprehensive performance, channels*

Introduction

The supercritical carbon dioxide (sCO_2) Brayton cycle system has captivated scholars` significant attention by virtue of the advantages of high effectiveness, compactness, alongside good economy. Functioning as one crucial part within the sCO_2 Brayton cycle, the heat exchanger plays a vital part in ensuring the stable operation of the entire cycle [1]. However, the conventional heat exchangers are not capable of meeting the demands of the Brayton cycle due to their inherent characteristics [2]. Due to their ability to adapt to the high temperature and pressure circumstance of the sCO_2 Brayton cycle, PCHE have become the focus of professionals and academics from all over the world.

The PCHE finds extensive applications not only in industrial waste heat recovery [3] and nuclear energy fields [4, 5] but also in various other areas, such as natural gas industry [6], hydrogen industry [7], and solar power plants [8]. In addition,with the development of compact electronic system, the cooling problem with high heat flux in the electronic system has attached much more attention [9]. At this point, a powerful heat dissipation or cooling system is

* Corresponding author, e-mail: wangyq@zzu.edu.cn

needed to ensure the reliability and service life of the electronic components [10]. Based on the structural characteristics of the flow channels, PCHE are generally classified into continuous and discontinuous flow channels [11]. Considerable research has been conducted by scholars globally to develop, explore, and optimize the flow channel structures of PCHE. Meshram *et al*. [12] compared performance of the most classic zigzag and straight flow channels and found that the mass-flow rate of the entering fluid significantly affects overall dimensions of PCHE. Chu *et al*. [13] obtained a series of experimental data for straight flow channels in sCO_2 Brayton cycles and derived empirical correlations with errors less than 7.2% for the transcritical conditions and errors less than 5.2% for the supercritical conditions. Xu *et al*. [14] conducted research on the cross-section of continuous flow channels and proposed an optimized rectangular cross-section based upon the traditional semicircular interface flow channel, significantly enhancing compactness of the PCHE. Zigzag flow channels and non-continuous *S*-shaped fins were the subjects of comparative experimental research by Ngo *et al*. [15]. Their findings showed that, for the same inlet Reynolds number, the zigzag flow channel's Nusselt number is 24-34% higher than that of *S*-shaped fins, however, that its pressure drop increases by 400-500%. Yang *et al*. [16] carried out relevant experimental research on PCHE with rhombic fins, and the final results showed that, at the identical volumetric heat transfer rate, pressure drop of the PCHE with rhombic fins only reaches 25% of that of the zigzag flow channel. Lin *et al*. [17] conducted a numerical analysis of the thermal performance and flow characteristics of PCHE with seven different continuous channels. The results indicate that the S-20 channel exhibits the best thermal performance. A set of airfoil fins with different groove thicknesses is designed by Ma *et al*. [18], the results show that, compared with the NACA0020 AFF, the AFF with a groove thickness of 0.6 mm reduce the pressure drop by up to 15% without affecting the thermal performance of the PCHE.

Impacts of local flow and heat transfer upon thermal-hydraulic PCHE performance with various channel configurations in pre-cooler circumstances has not yet been fully understood, despite the fact that substantial study has been done on the thermodynamic properties of sCO_2 flow in PCHE [19]. Therefore, comprehending the performance distinctions in disparate categories of PCHE is of great significance [20]. Moreover, compared to the abundant analysis, research, and optimization of PCHE with continuous flow channels by experts and scholars, limited studies have delved into the case of PCHE with discontinuous flow channel configurations in pre-cooler conditions. Therefore, based on the practical application of marine sCO_2 Brayton cycle systems applied to electricity generation, this study compares and analyzes three typical discontinuous flow channels: rhombic fin channel [16], airfoil fin channel [21], and rectangular fin channel [11]. Through the analysis concerning heat transfer performance, flow performance, alongside overall performance of three channels, distinctive characteristics of each channel are determined, providing important practical guidance for future studies and advancement of sCO_2 Brayton cycle pre-coolers if marine applications. Additionally, by conducting in-depth research on PCHE performance under pre-cooler conditions, focusing on heat transfer and local flow effects, enhances the understanding of PCHE performance. This research establishes a significant theoretical basis for improving and optimizing PCHE design and application.

Numerical model and boundary conditions

Physical model

Flow channels of PCHE are very small in size, but their quantity can be enormous, reaching millions in numbers. Considering the convenience and feasibility of model calcula-

tions, it is common simplify the overall model of PCHE into a single heat transfer and flow unit structure [22]. On account of the long axial length of flow channels, fig. 1 illustrates the local regions of the simplified models for the three types of flow channels.

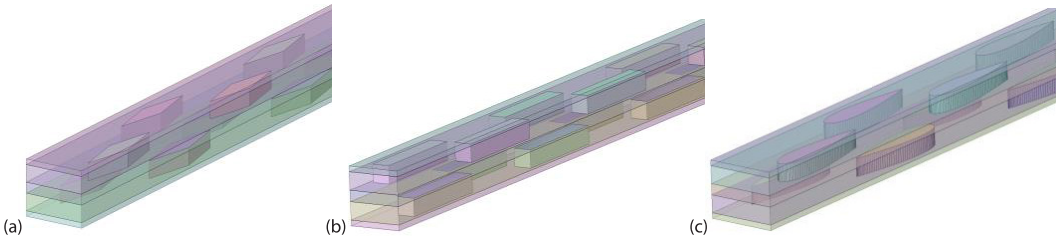

Figure 1. Schematic diagram of a simplified model of PCHE; (a) rhombic fin channel, (b) rectangular fin channel, and (c) airfoil fin channel

The lengths of the three types of flow channels were based on the geometric parameters from Liu *et al.* [23], and were all set to 292 mm. The flow directions of hot and cold fluids were counterflow. When arranging the airfoil flow channel, care was taken to ensure that the fins of the cold and hot flow channels were oriented in opposite directions. With the objective of ensuring periodic assumption of the PCHE model, except for these planes where inlets of hot and cold fluids are located, all other surfaces are set as periodic walls. The number, thickness, length, and height of fins within each channel are the same. Here, the rectangular channel is used as an example for specific explanation, as shown in fig. 2.

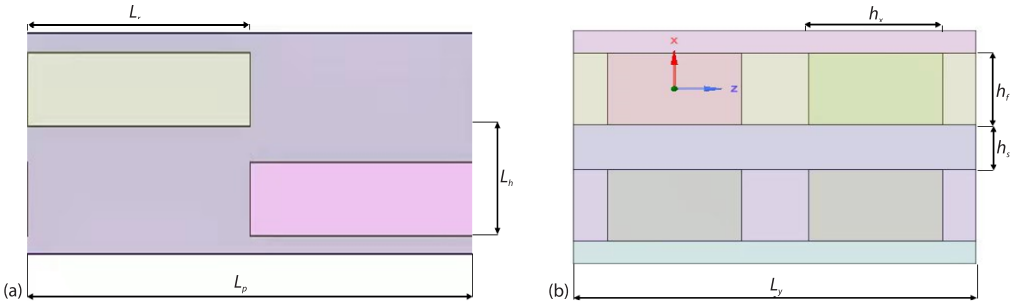

Figure 2. Detailed geometric model illustration; (a) top view and (b) front view

When constructing the geometric model of the channel, the geometric parameters of Jin *et al.* [19] are referenced. The height, length, and thickness of each fin are set as $h_f = 0.8$ mm, $L_r = 6$ mm, $h_x = 1.2$ mm, respectively. Lateral distance between fins is set as $L_h = 1.8$ mm. Additionally, the longitudinal distance is designed to be 12 mm. As for the heat transfer unit, its width and plate thickness are also consistent with the parameters of [19], set as $L_y = 3.6$ mm and $h_s = 0.5$ mm, respectively.

Boundary conditions and governing equations

During the numerical simulation using FLUENT software, considering the practical scenario of waste heat recovery in marine exhaust, the boundary conditions adopted by Liu *et al.* [23] were referenced. Inlet temperature of the cold fluid was designated to be 298.15 K, and inlet temperature of the hot fluid (sCO_2) was set to 333 K. Additionally, Liu *et al.* [23] discovered that PCHE performs better as a pre-cooler in high Reynolds number and elevated pressure circumstances. Hence, this hot fluid outlet pressure was set to 9.5 MPa, and the inlet

Reynolds number was set to 23000. For the cold fluid, the outlet pressure was designed to be 0.15 MPa. In addition, the inlet Reynolds number was set to 980. For the non-continuous flow channels of airfoil fins, these conditions corresponded to a hot fluid inlet mass-flow rate of 0.00121 kg/s and a cold fluid inlet mass-flow rate of 0.00225 kg/s. In order to have a more intuitive comparison and evaluation of heat transfer performance, flow performance, alongside overall performance of three types of flow channels, the boundary conditions suggested by Aneesh *et al*. [24] were used. Cold and hot fluid inlet mass-flow rates for rhombic and rectangular fin channels were also set to 0.00121 kg/s and 0.00225 kg/s, respectively. For greater clarity, tab. 1 lists the specific boundary conditions used in the numerical simulation. The solid material selected for the study was 316 L [19], which is a corrosion-resistant alloy known for its excellent performance in various industrial applications. To ensure the accuracy of the thermophysical properties of sCO_2, all thermal properties of sCO_2 originated in the NIST standard reference database 23 (REFPROP) [25]. Furthermore, Palko *et al*. [26] discovered that the SST *k-ε* turbulence model provides great accuracy of estimating behaviors of heat transport and flow in supercritical fluids. Accordingly, the aforementioned model was applied to the current calculations. The SIMPLE algorithm in FLUENT is a steady-state numerical method commonly employed for solving fluid dynamics problems. It utilizes an iterative approach to couple the pressure and velocity fields, gradually converging to a consistent solution. The algorithm ensures the satisfaction of the mass conservation equation and is widely applicable in various fluid-flow scenes. So the SIMPLE algorithm was utilized to solve the velocity-pressure coupling relationship. Additionally, one second-order upwind scheme was applied to discretize the governing equations during ANSYS FLUENT software calculations.

The governing equations are depicted:

Continuity equation: $\dot{m}_{\mathrm{h,in}}$ [gs^{-1}] and $\dot{m}_{\mathrm{c,in}}$ [gs^{-1}]:

$$\frac{\partial(\rho u)}{\partial x}+\frac{\partial(\rho v)}{\partial y}+\frac{\partial(\rho w)}{\partial z}=0 \tag{1}$$

where u, v, and w [ms^{-1}] are the velocity components in x, y, and z orientations.

Momentum equation:

$$\rho\frac{\partial(u_i u_j)}{\partial x_j}=-\frac{\partial p_i}{\partial x_i}+\mu\frac{\partial}{\partial x_j}\left(\frac{\partial u_i}{\partial x_j}+\frac{\partial u_j}{\partial x_i}-\frac{2}{3}\delta_{ij}\frac{\partial u_k}{\partial x_k}\right) \tag{2}$$

where p [Pa] is the pressure and ν [m^{2}s^{-2}] – the fluid kinematic viscosity.

Energy equation:

$$u\frac{\partial T}{\partial x}+v\frac{\partial T}{\partial y}+w\frac{\partial T}{\partial z}=\frac{\lambda}{\rho c_p}\left(\frac{\partial^2 T}{\partial x^2}+\frac{\partial^2 T}{\partial y^2}+\frac{\partial^2 T}{\partial z^2}\right) \tag{3}$$

where ρ [kgm^{-3}] is the fluid density, c_p [Jkg^{-1}K^{-1}] – the fluid thermal capacity, and λ [Wm^{-1}K^{-1}] – the fluid's thermal conductivity.

Solid's Governing equation:

$$\frac{\partial}{\partial x}\left(\lambda_s\frac{\partial T}{\partial x}\right)+\frac{\partial}{\partial y}\left(\lambda_s\frac{\partial T}{\partial y}\right)+\frac{\partial}{\partial z}\left(\lambda_s\frac{\partial T}{\partial z}\right)=0 \tag{4}$$

where λ_s [Wm^{-1}K^{-1}] is the solid material's thermal conductivity and T [K] – the solid element's temperature.

Due to the width of the flow channel changes along the flow direction, the following equation is used to calculate the hydraulic diameter:

$$D_h = \frac{4V_h}{S} \tag{5}$$

where V_h is the volume of the fluid domain and S – the area of the coupled walls between the fluid and solid.

The Reynolds number, is expressed:

$$\mathrm{Re} = \frac{\dot{m}D_h}{\mu(V_h - L)} \tag{6}$$

where $\dot{m}$ is the inlet mass-flow rate of fluid, μ – the dynamic viscosity of the fluid, and L – the length of the fluid.

Grid partitioning and numerical model validation

Considering various geometric factors of non-continuous flow channels, the time and quantity for grid partitioning, ANSYS FLUENT MESHING software was used to generate polyhedral grids for three types of non-continuous flow passages in PCHE. Additionally, near the fluid-solid interface, grid refinement techniques were employed to partition the boundary-layer grids. Grid independence analysis was conducted on airfoil fin channel, rectangular fin channel, and rhombic fin channel, fig. 3. It was observed that when the grid quantity was over two million, that is, when the grid size varied within the range of 0.1-0.16 mm, the variation of performance parameters was relatively stable. Therefore, grid models within this size range were selected for subsequent simulation analysis.

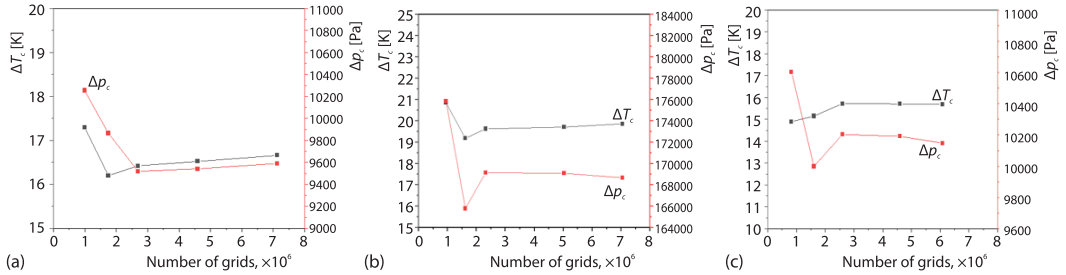

Figure 3. Grid independence analysis of different channels; (a) airfoil fin channel, (b) rectangular fin channel, and (c) rhombic fin channel

Table 1. List of some boundary conditions

Boundary condition value of number	Value of number	Boundary condition value of number	Value of number
$T_{h,in}$ [K] 333	333	$T_{c,in}$ [K] 298.15	298.15
$p_{h,out}$ [MPa] 9.5	9.5	$p_{c,out}$ [MPa] 0.15	0.15
$\dot{m}_{h,in}$ [gs^{-1}] 0.00121	0.00121	$\dot{m}_{c,in}$ [gs^{-1}] 0.00225	0.00225

To validate the reliability of calculating thermal-hydraulic PCHE performance within this research, experimental models, conditions, and results mentioned by Liu *et al*. [23] in their numerical model validation of PCHE as a pre-cooler were employed, the experimental boundary conditions are as shown in tab. 1, and the experimental results are represented by the hot fluid outlet temperature, as detailed in fig. 4, corresponding to the simulated outlet temperature results. The operating conditions in the cited references were closely matched with those used in this study, and the resulting variations inside the thermal properties of working fluid were

also similar. Thus, the references provided a good basis for comparison. when analyzing the experimental data, the author considered both the inlet and outlet pressures of the cold fluid (water) as atmospheric pressure, with a pressure drop of 0 Pa. Additionally, for the sake of experimental rigor, the pressure drop on the side of the cold fluid can be considered negligible compared to the pressure drop of the hot fluid. Five out of the seven experimental sets from the references were selected for numerical validation [22]. Table 2 lists the experimental conditions used in the five groups of experiments in the references.

Table 2. Boundary conditions for numerical model validation

$\dot{m}_{c,in}$ [gs^{-1}]	$\dot{m}_{h,in}$ [gs^{-1}]	$p_{c,out}$ [MPa]	$p_{h,out}$ [MPa]	$T_{c,in}$ [K]	$T_{h,in}$ [K]
0.6053	0.3612	0	8.63	297.15	312.85
0.5763	0.3073	0	8.70	297.15	318.70
0.2352	0.2381	0	8.92	298.15	312.02
0.0253	0.0897	0	8.41	293.15	320.57
0.0028	0.0464	0	9.32	289.15	328.70

During the numerical simulation, the physical model was simplified, periodic boundary conditions were set, and the same calculation methods as those for the three flow passages in the previous sections were adopted. Temperature difference of the hot fluid was selected as parameters for comparison. The simulation results are shown in fig. 4. As depicted in fig. 4, Under the condition of ensuring the consistency of numerical simulation and experimental boundary conditions, the final outlet temperatures of the hot fluid for different outlet pressures, inlet temperatures, and inlet mass-flow rates in both numerical simulation and experiments are shown in the figure below. The magnitudes of their relative errors are all within one percent. This validates the numerical model employed in this research to calculate heat transfer and flow PCHE parameters.

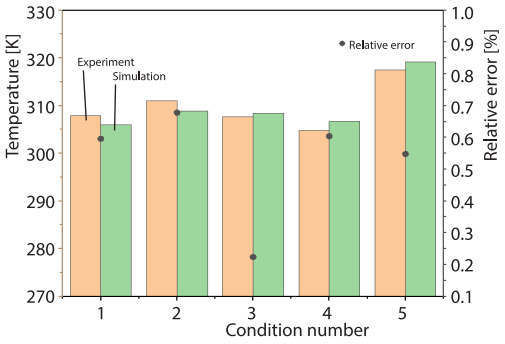

Figure 4. Comparison of experimental and simulation results

Analysis on simulation results

Flow performance analysis of different fin channels

The introduction of the relative helicity, H_r, is used to analyze the flow pattern along the flow path and further understand the pressure loss characteristics during fluid-flow. The angle between velocity and vorticity vectors is denoted by H_r. The H_r could be used to determine the condition of vortices in turbulent flow [27]:

$$H_r = \frac{v\omega}{|v||\omega|} \tag{7}$$

where ω is the vorticity, which is the curl of the velocity vector in s^{-1}:

$$\omega = \nabla v \tag{8}$$

According to eq. (7), the value of H_r always lies between –1 and 1. When H_r is greater than 0, it indicates that the angle between velocity and vorticity vectors is less than 90°. As to

the vortex, the rotation orientation is opposite to the fluid-flow orientation. When H_r is less than 0, it indicates that the angle between velocity and vorticity vectors is greater than 90°, and the rotation direction of the vortex is the same as the fluid-flow direction. Figure 5 presents the distribution contour maps and streamlines of the relative helicity at positions x = 5 mm, x = 11.7 mm, x = 18.4 mm, and x = 25 mm for the three channels.

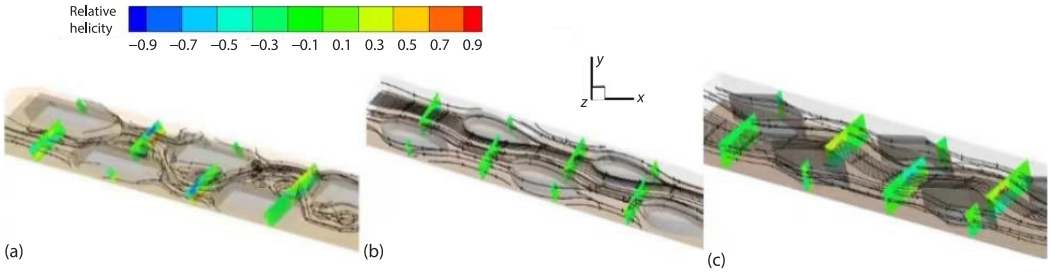

Figure 5. Distribution contour maps and streamline plots of H_r at different locations for the three fin channels; (a) rectangular fin channel, (b) air-foil fin channel, and (c) rhombic fin channel

From fig. 5, it can be observed that the relative helicity in the airfoil and rhombic fin channels is closer to 0, indicating more stable flow and fewer vortex regions in these two channels. However, in the rectangular fin channel, there is a larger area with relative helicity significantly deviating from 0. This is because as the fluid-flows over the front surface of the rectangular fin, a rigid transition occurs, leading to the formation of a large number of vortices in the rectangular channel and resulting in higher along-channel pressure loss.

According to fig. 6, the pressure variation along the flow path is relatively uniform for all three types of non-continuous fin channels, but there are significant differences in the total pressure drop. The rectangular fin channel exhibits highest pressure drop, which is approximately 16.6 times and 17.8 times higher than the pressure drops of the rhombic and airfoil fin channels, respectively. This is due to the fact that the pressure loss in the heat exchanger primarily consists of along-channel pressure loss and local pressure loss. Compared to the airfoil and rhombic fin channels, in the rectangular fin channel, the fluid-flow is hindered when it passes through the junction of the two fins, directly impacting the rectangular surface of the next fin. This phenomenon leads to a significant local pressure loss. In this regard, the streamlined structure of airfoil fins and the gradually varying structure of rhombic fins ensure that fluid-flow does not undergo abrupt changes along the flow direction. Therefore, the local pressure loss in these channels is much smaller than that in the rectangular fin channel.

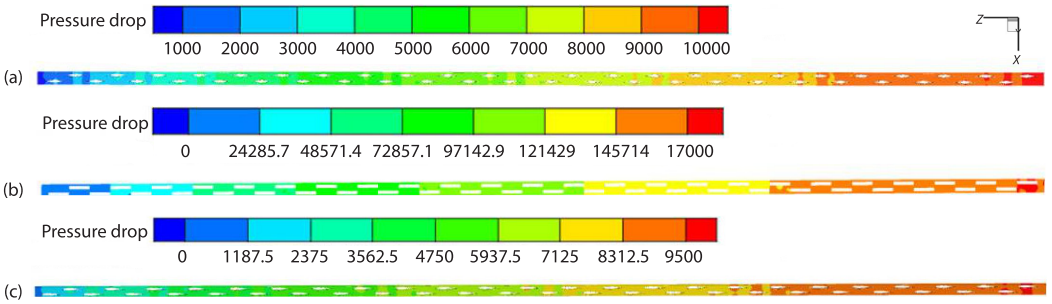

Figure 6. Pressure drop contour maps for different fin channels; (a) rhombic fin channel, (b) rectangular fin channel, and (c) air-foil fin channel

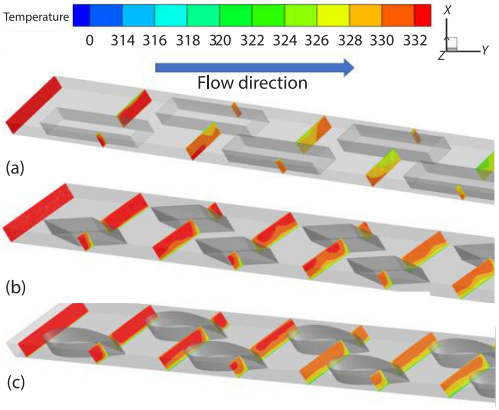

Figure 7. Temperature contour maps at different locations in the three flow channels; (a) rectangular fin channel, (b) rhombic fin channel, and (c) air-foil fin channel

Heat transfer performance analysis of disparate fin channels

With the intention of accurately comparing the heat transfer capabilities of different non-continuous fin channels in PCHE, fig. 7 presents temperature contour maps of the three channels at distances of 8 mm, 12 mm, 16 mm, and 20 mm from the inlet in the hot fluid region, using the same scale. By observing the color distribution in the figures, it can be noticed that the rectangular channel exhibits significantly more orange and light yellow regions on various cross-sections as compared to the other two channels. This indicates that fluid temperature within the rectangular channel is lower, compared to that in other two channels. This is due to the structural differences of the rectangular channel as compared to the other two channels, resulting in a rigid transition of the fluid as it passes through the rectangular interface opposite to the flow direction. This intensifies the turbulent mixing between the fluid layers and thereby enhances the convective heat transfer.

Figure 8 illustrate temperature changes along the flow path and comparison of coefficients of the local convective heat transfer for different channels in PCHE. As shown in fig. 8(a), the hot fluid enters all three channels at the same temperature, but there are differences in the outlet temperatures. The rectangular fin channel exhibits the largest temperature drop, with a reduction of 3.9 K and 3.2 K as compared to the airfoil and rhombic fin channels, respectively. Additionally, it could be observed that temperature rate decrease along the flow direction varies for the three channels. This phenomenon is consistent with Lv *et al.* [28] finding that temperature distribution of the hot fluid within a pre-cooler is initially relatively steep and then gradually becomes much smoother along the flow orientation. This is mostly on account of a

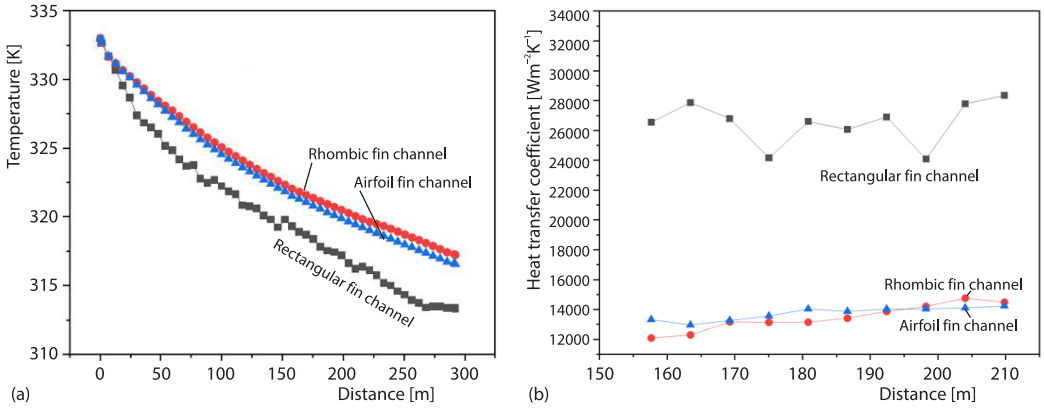

Figure 8. Temperature change along the flow path and local convective heat transfer coefficient comparison; (a) temperature change along the flow path and (b) local convective heat transfer coefficient comparison

significant improvement in the thermal capacity of the fluid from inputs to outlets, resulting in improved heat transfer capacity and lower temperature variations per unit length. According to fig. 8(b), the rectangular fin channel has a much greater local convective heat transfer coefficient, as compared with airfoil and rhombic fin channels. Air-foil fin and rhombic fin channels have similar coefficients of local convective heat transfer, but the airfoil fin channel shows a slightly higher trend in overall values. This difference is attributed to the flow in per channel. Within the rectangular fin channel, the fluid directly impacts the fin surfaces, resulting in the strongest disturbance and highest level of convective heat transfer. On the other hand, the airfoil fin and rhombic fin channels exhibit a streamlined and gradually varying structure, which minimizes turbulence and consequently reduces the convective heat transfer. The distinctive flow patterns in each channel lead to varying degrees of convective heat transfer, with the rectangular fin channel exhibiting highest local heat transfer coefficients by virtue of its direct flow impact on fins, while the airfoil fin and rhombic fin channels demonstrate relatively weaker convective heat transfer as a result of their streamlined and less turbulent flow characteristics.

Comprehensive performance analysis of different fin channels

Based upon the consequences in figs. 9 and 10, the comprehensive performance of the three channels in the PCHE can be evaluated.

According to fig. 9, regardless of the inlet mass-flow rate, the order of Nu/f [29] values for the three channels is airfoil fin channel PCHE > rhombic fin channel PCHE > rectangular fin channel PCHE. Additionally, the Nu/f value for the rhombic fin channel PCHE is relatively close to that of the airfoil fin channel PCHE but consistently lower. When comparing to the rectangular fin channel PCHE at the identical inlet mass-flow rate, comprehensive performance of the rhombic fin channel PCHE becomes higher by 153.59%, 391.9%, and 249.2%, respectively, while overall performance of the airfoil fin channel PCHE is higher by 172.1%, 443.97%, and 274.75%, respectively.

According to fig. 10, for three different mass-flow rates, the comparison of $Q/\Delta p$ values yields consistent results with the first evaluation method. It also indicates that under the same pressure drop, the airfoil fin channel PCHE can transfer more heat, heat transfer performance of the rhombic fin channel PCHE is similar but mildly lower than that of the airfoil fin channel PCHE, while performance of the rectangular fin channel PCHE is far inferior to the other two channels. Furthermore, from fig. 10, it can be observed that the $Q/\Delta p$ values of the rectangular and rhombic fin channels tend to approach those of the airfoil fin channel with the

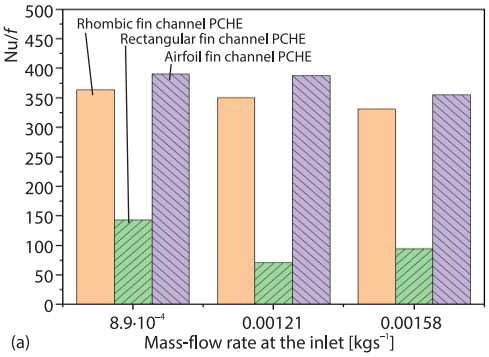

Figure 9. The Nu/f values for different fin channels

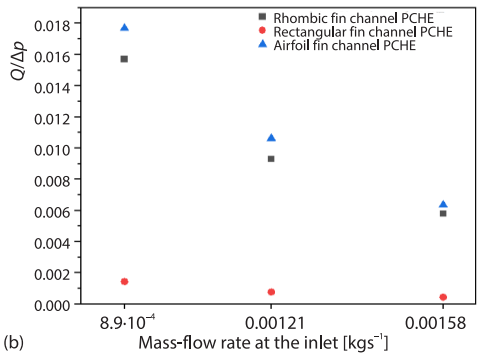

Figure 10. The $Q/\Delta p$ values for different fin channels

increase of the inlet mass-flow rate, and these $Q/\Delta p$ values of all three channels decrease with the increase of the inlet mass-flow rate.

To sum up, the airfoil fin channel PCHE exhibits the optimal comprehensive performance, followed by the rhombic fin channel PCHE, while the rectangular fin channel PCHE performs the worst.

Conclusions

The study utilized CFD method to perform numerical simulations on various non-continuous flow passage PCHE operating as pre-coolers within one marine sCO_2 Brayton cycle system for electricity generation under typical conditions. The research yielded the following conclusions, as well as recommendations for enhancing PCHE performance.

- *Flow performance*: Air-foil fin-channels demonstrate the optimal flow performance on account of the unique streamlined structure, allowing for smoother fluid-flow through the channel. The rhombic fin-channel operates slightly worse, while rectangular fin-channel exhibits the poorest flow performance with higher pressure drop during the flowing.
- *Heat transfer performance*: Rectangular fin-channel PCHE exhibit the best heat transfer performance, followed by airfoil fin-channels, while rhombic fin channels shows relatively poorer heat transfer performance. Additionally, the temperature drop rate in all three channels decreases in the orientation of the fluid-flow.
- In the identical inlet mass-flow rate for three channels, by comparing the Nu/f values and $Q/\Delta p$ values, the same ranking of comprehensive performance is obtained: air-foil fin-channel PCHE > rhombic fin-channel PCHE > rectangular fin-channel PCHE. At the same inlet mass-flow rate, compared to the rectangular fin channel PCHE, the comprehensive performance of the rhombic fin channel PCHE increased by 153.59%, 391.9%, and 249.2%, while the comprehensive performance of the airfoil fin channel PCHE increased by 172.1%, 443.97%, and 274.75%.This indicates that though rectangular fin-channels have the highest heat transfer capability, it comes at a significant cost of pressure drop.
- Due to the significant variation in fluid properties when sCO_2 flows in the pre-cooler, there is a substantial difference in heat transfer and local flow performance from inlets to outlets. Therefore, based on the superior overall performance of airfoil fin-channels, it`s suggested to propose one new channel lay-out by modifying the fin spacing or fin size, using the concept of partitioned enhanced heat transfer, to achieve high efficiency and low resistance.

In conclusion, The initial research primarily focused on the isolated analysis of a discontinuous flow channel, lacking understanding of the inherent strengths and weaknesses of different channels. There was a deficiency in cross comparisons. Additionally, there is limited research on utilizing sCO_2 Brayton cycle power generation systems to recover waste heat from ship exhausts. The innovation of this paper lies in its dedicated focus on the practical application of utilizing waste heat from ship exhausts. Through a comparative analysis of the characteristics of three typical channels, we gained a clear understanding of the flow and heat transfer characteristics of each channel. Based on this, we proposed the channel with the best overall performance and ultimately identified the structure most suitable for practical scenarios.

Acknowledgment

This work is supported by National Natural Science Foundation of China (Grant No. 21776263).

Nomenclature

c_p – thermal capacity, [Jkg^{-1}K^{-1}]
D_h – hydraulic diameter, [m]
f – friction factor [=$\Delta p D_h/2\rho u^2 L$], [–]
H_r – relative helicity, [l]
h – heat transfer coefficient, [Wm^{-2}K^{-1}]
h_f – height of fins
h_s – plate thickness, [mm]
L_r – length of fins
$\dot{m}$ – mass-flow rate, [kgs^{-1}]
$\dot{m}_{c,in}$ – cold fluid inlet mass-flow rate, [kgs^{-1}]
$\dot{m}_{h,in}$ – hot fluid inlet mass-flow rate, [kgs^{-1}]
Nu – Nusselt number, [=$QD_h/(T_w - T_f)\lambda$], [–]
p – pressure, [MPa]
$p_{c,out}$ – cold fluid outlet pressure, [MPa]
$p_{h,out}$ – hot fluid outlet pressure, [MPa]
Δp – pressure drop, [Pa]
Q – heat transfer rate, [W]
Re – Reynold number, [= $mD_h/\mu/(V_h/L)$], [–]
T – temperature, [K]
ΔT – temperature difference, [K]
$T_{c,in}$ – cold fluid inlet temperature, [K]
$T_{h,in}$ – hot fluid inlet temperature, [K]

Greek symbols

μ – dynamic viscosity, [Pa·s]
ν – kinematic viscosity, [m^{2}s^{-1}]
ρ – density, [kgm^{-3}]

Subscripts

f – fluid
in – inlet
out – outlet
w – wall

Acronyms

NIST – national institute of standards and technology
PCHE – printed circuit heat exchanger

References

[1] Ming, Y., *et al*., Dynamic Modelling and Validation of the 5 MW small Modular Supercritical CO_2 Brayton-Cycle Reactor System, *Energy Conversion and Management*, *253* (2022), 115184
[2] Jin, S. K., *et al*., Compact Heat Exchangers for Supercritical CO_2 Power Cycle Application, *Energy Conversion and Management*, *209* (2020), 112666
[3] Yan, X. P., *et al.*, Review on sCO_2 Brayton Cycle Power Generation Technology Based un Ship Waste Heat Recovery Utilization, *China Mechanical Engineering*, *30* (2019), pp. 939-946
[4] Bai, J., *et al*., Numerical Investigation on Thermal Hydraulic Performance of Supercritical LNG in Sinusoidal Wavy Channel Based Printed Circuit Vaporizer, *Applied Thermal Engineering*, *175* (2020), 115379
[5] Lee, Y., Lee, J. I., Structural Assessment of Intermediate Printed Circuit Heat Exchanger for Sodium-Cooled Fast Reactor with Supercritical CO_2 Cycle, *Annals of Nuclear Energy*, *73* (2014), Nov., pp. 84-95
[6] Pan, J., *et al*., Numerical Investigation on Thermal-Hydraulic Performance of a Printed Circuit LNG Vaporizer, *Applied Thermal Engineering*, *165* (2020), 114447
[7] Cheng, Y., *et al*., Multi-Objective Optimization of Printed Circuit Heat Exchanger Used for Hydrogen Cooler by Exergoeconomic Method, *Energy*, *262* (2023), 125455
[8] Shi, H. Y., *et al.*, Heat Transfer and Friction of Molten Salt and Supercritical CO_2 Flowing in an Air-foil Channel of a Printed Circuit Heat Exchanger, *International Journal of Heat and Mass Transfer*, *150* (2020), 119006
[9] Chu, W. X., *et al*., Heat Transfer and Pressure Drop Performance of Printed Circuit Heat Exchanger with Different Fin Structures, *Chinese Science Bulletin*, *62* (2017), 16, pp.1788-1794
[10] Morteza, *et al*., Numerical Analysis of Heat Transfer and Flow Characteristics of Supercritical CO_2-Cooled Wavy Mini-Channel Heat Sinks, *Applied Thermal Engineering*, *226* (2023), 120307
[11] Xu, X. Y., *et al*., Thermal-Hydraulic Performance of Different Discontinuous Fins Used in a Printed Circuit Heat Exchanger for Supercritical CO_2, *Numerical Heat Transfer Part A Applications*, *68* (2015), 10, pp. 1067-1086
[12] Meshram, A., *et al*., Modelling and Analysis of a Printed Circuit Heat Exchanger for Supercritical CO_2 Power Cycle Applications, *Applied Thermal Engineering*, *109* (2016), Part B, pp. 861-870
[13] Chu, W. X., *et al*., Experimental Investigation on sCO_2-Water Heat Transfer Characteristics in a Printed Circuit Heat Exchanger with Straight Channels, *International Journal of Heat and Mass Transfer*, *113* (2017), Oct., pp. 184-194
[14] Xu, Z. R., *et al.*, Study on Mechanical Stress of Semicircular and Rectangular Channels in Printed Circuit Heat Exchangers, *Energy*, *238* (2022), 121655

[15] Ngo, T. L., *et al*., Heat Transfer and Pressure Drop Correlations of Micro-Channel Heat Exchangers with S-Shaped and Zigzag Fins for Carbon Dioxide Cycles, *Experimental Thermal and Fluid Science*, *32* (2007), 2, pp. 560-570
[16] Yang, Y., *et al.*, Experimental Study of the Flow and Heat Transfer Performance of a PCHE with Rhombic Fin Channels, *Energy Conversion and Management*, *254* (2022), 115137
[17] Lin, Y. S., *et al*., Numerical Investigation on Thermal Performance and Flow Characteristics of Z and S Shape Printed Circuit Heat Exchanger Using S-CO_2, *Thermal Science*, *23* (2019), Suppl. 3, pp. S757-S764
[18] Ma, Y., *et al*., Performance Study on a Printed Circuit Heat Exchanger Composed of Novel Airfoil Fins Fsupercritical CO_2 Cycle Cooling System, *Thermal Science*, *27* (2022), 1B, pp. 891-903
[19] Jin, F., *et al*., Thermo-Hydraulic Performance of Printed Circuit Heat Exchanger as Precooler in Supercritical CO_2 Brayton Cycle, *Applied Thermal Engineering*, *210* (2022), 118341
[20] Pidaparti, S. R., *et al.*, Experimental Investigation of Thermal-Hydraulic Performance of Discontinuous Fin Printed Circuit Heat Exchangers for Supercritical CO_2 Power Cycles, *Experimental Thermal and Fluid Science*, *106* (2019), Sept., pp. 119-129
[21] Chu, W. X., *et al*., Thermo-Hydraulic Performance of Printed Circuit Heat Exchanger with Different Cambered Air-Foil Fins, *Heat Transfer Engineering*, *41* (2019), 8, pp. 1-14
[22] Gao, Y. C., *et a*l., Study on the Effects of Channel Width and Fin Angle on Heat Transfer and Pressure Drop of Zigzag PCHE, *Journal of Engineering for Thermal Energy and Power*, *34* (2019), pp. 94-100
[23] Liu, B. H., *et al*., Thermal-Hydraulic Performance Analysis of Printed Circuit Heat Exchanger Precooler in the Brayton Cycle for Supercritical CO_2 Waste Heat Recovery, *Applied Energy*, *305* (2022), 117923
[24] Aneesh, M. A., *et al*., Thermal-Hydraulic Characteristics and Performance of 3-D Straight Channel Based Printed Circuit Heat Exchanger, *Applied Thermal Engineering*, *98* (2016), Apr., pp. 474-482
[25] Lemmon, E. W., *et al*., The NIST Standard ReferenceDatabase 23: Reference Fluid Thermodynamic and Transport Properties-REFPROP. 9.0. NIST NSRDS, 2010
[26] Palko, D., H. Anglart, H., Theoretical and Numerical Study of Heat Transfer Deterioration in High Performance Light Water Reactor, *Science and Technology of Nuclear Installations*, *2008* (2008), ID405072
[27] Moffatt, H. K., Tsinober, A., Helicity in Laminar and Turbulent Flow, *Annual Review of Fluid Mechanics*, *24* (1992), Jan., pp. 281-312
[28] Lv, Y. G., *et al*., Numerical Investigation on Thermal Hydraulic Performance of Hybrid Wavy Channels in a Supercritical CO_2 Precooler, *International Journal of Heat and Mass Transfer*, *181* (2021), 121891
[29] Fan, J. F., *et al.*, A Performance Evaluation Plot of Enhanced Heat Transfer Techniques Oriented for Energy-Saving, *International Journal of Heat and Mass Transfer*, *52* (2009), 1-2, pp. 33-44

Paper submitted: September 2, 2023
Paper revised: January 4, 2024
Paper accepted: January 23, 2024